Neural Computing and Applications (2022) 34:12845–12859
https://doi.org/10.1007/s00521-022-07149-w

ORIGINAL ARTICLE

A utilization of the inverse response surface method for the reliability-based design of structures

David Lehký[1] · Martina Šomodíková[1] · Martin Lipowczan[1]

Received: 2 December 2021 / Accepted: 28 February 2022 / Published online: 23 March 2022

Abstract
This paper discusses the pitfalls of using response surface methods when solving inverse problems and presents an adaptive artificial neural network-based inverse response surface method. The procedure is based on a coupling of the adaptive response surface method and artificial neural network-based inverse reliability analysis. The validity and accuracy of the method are tested on several examples. The first is a problem with a theoretical explicit nonlinear limit state function and one design parameter. Here, the accuracy of surrogate models for design parameter identification was tested for cases with the target values of the identified parameter both inside and outside of the initial range of values. The absolute percentage errors were 11.79 % and 0.19 % after the first and the last iteration of the identification process, respectively. The other two examples represent practical applications of the reliability design of structures with multiple design parameters and multiple reliability constraints. In the former, the limit state functions are defined explicitly, while in the latter, they are defined implicitly in the form of a structural analysis using the nonlinear finite element method. When assessing the reliability index values, very low absolute percentage error values were obtained in both examples. For the explicit form of the limit state function, the values were up to 0.50 % in all iterations. In the case of the implicitly defined limit state function, the absolute percentage error was equal to 6.45 % after the fist iteration and 0.79 % after the second iteration.

Keywords Response surface · Inverse response surface method · Artificial neural network · Inverse reliability analysis · Reliability-based design · Failure probability

1 Introduction

Probabilistic reliability analysis is a suitable approach that allows one to take the uncertainties (in material properties, loads, geometrical imperfections, etc.) that are inherently present in a structure–load–environment system and incorporate them into reliability calculations, and then to quantify the resulting reliability. The quantification is performed using reliability indicators, most often in the form of failure probabilities of the limit state being analysed. The explicit calculation of the probability integral is generally impossible. In practice, the calculation of failure probability is solved exclusively using numerical methods of either the simulation or approximation type.

Simulation methods, such as the Monte Carlo method, Latin hypercube sampling, and importance sampling, are inherently close to the general perception of probability and so are very popular in practical applications [1, 2]. However, by their very nature, they require the execution of a relatively large number of simulations, i.e. the repeated evaluation of the mathematical model. However, the model tends to be quite complex and computationally demanding in many practical engineering applications, e.g. the solution of a structure via the nonlinear finite element method (NLFEM). This entails extreme time demands, especially when it is necessary to perform repeated reliability analyses, e.g. when solving reliability-based design optimisation tasks or performing global sensitivity analyses where thousands of runs are required [3, 4]. Thus, in many of these cases, it is necessary to employ one of the approximation methods available. Traditional approximation methods include the first-order reliability method (FORM) [5] and the second-order reliability method (SORM) [6].

✉ David Lehký
lehky.d@fce.vutbr.cz

[1] Faculty of Civil Engineering, Brno University of Technology, Veveří 331/95, 602 00 Brno, Czech Republic

With the recent development of metamodelling and the use of soft computing methods, the response surface method [7–10] is becoming a very popular approximation method suitable for solving reliability in the context of complex engineering problems. Promising examples include response surfaces based on polynomial chaos expansion [11], support vector machines [12] and Kriging metamodels [13–15]. When dealing with unbalanced data, ensemble models can help to improve accuracy by combining several base estimators. Multiple weak estimators can be merged with adaptive boosting to create a single strong estimator [16]. Deep learning neural networks, such as convolutional neural networks and long-short term memory networks, show exceptional capabilities in improving the accuracy of classical machine learning approaches [17, 18].

The whole problem becomes a bit more complicated when solving the inverse reliability problem. Its aim is usually to determine the "design parameters" (material properties, dimensions, amount of reinforcement, etc.) for the required reliability indicators. In the case of a deterministic problem, the trial-and-error method is commonly used in practice, but its insufficiency is obvious in the case of a probabilistic solution. In these cases, more advanced methods need to be employed, e.g. a reliability contour method [19, 20], an iterative algorithm based on the modified Hasofer-Lind-Rackwitz-Fiessler scheme used in reliability analysis [21], a Newton-Raphson iterative algorithm employed to find multiple design parameters [22, 23], a decomposition technique [24], or various implementations of artificial neural networks (ANN) with other soft-computing techniques [25–28].

When solving inverse reliability problems in practice, the quantification of reliability indicators is often simplified by using the FORM method, which corresponds to a linear approximation of the limit state function. However, this can lead to considerable inaccuracy in the estimation of reliability indicators when solving nonlinear problems and, consequently, to poor estimates of design parameters. So, naturally, the response surface method with a nonlinear surrogate model is suggested. In order to construct the response surface, the values of all variables need to be known. However, this is not possible in the case of an inverse problem where design parameters are the subject of identification. In most cases, the response surface is constructed for the initial estimation of the design parameters. The subsequent inverse analysis may then result in inaccurate design parameter estimates. Their accuracy depends on a number of aspects, such as the number of design parameters, the quality of their initial estimation and the shape of the limit state function. This inaccuracy is further accentuated by approximating the limit state function around the mean values. However, let us not forget that the accuracy of the failure function approximation in the failure region is crucial for the correct estimation of the failure probability. Both of these aspects are addressed by the inverse response surface method introduced in this paper. It is an adaptive method that progressively refines the response surface approximation in the failure region and thus the estimation of the design parameters.

The presented methodology is closely related to the authors' previous work on the reliability calculation of time-consuming problems using a small-sample ANN-based response surface method [29] and an ANN-based inverse reliability method [28]. In the following section, both methods will be briefly described. Section 2.4 then introduces the proposed inverse response surface method. Numerical examples, a discussion of the results and a summary of the main aspects of the application follow.

2 Methods

2.1 Reliability problem formulation

The aim of classical (forward) reliability analysis is the estimation of unreliability using a reliability indicator called the theoretical failure probability, defined as:

$$p_{\mathrm{f}} = P(Z \leq 0), \tag{1}$$

where $Z = g(\mathbf{X})$ is a variable called "safety margin", which is a function of a random vector, $\mathbf{X} = \{X_1, X_2, \ldots, X_n\}^T$, where n is the number of random variables. Random vector $\mathbf{X}$ follows a joint probability distribution function (PDF) $f_{\mathbf{X}}(\mathbf{x})$; in general, its marginal variables can be statistically correlated. The classical approach deals with situations where the information about $f_{\mathbf{X}}(\mathbf{x})$ is limited to knowledge of univariate marginal distributions $f_{X_1}(x), \ldots, f_{X_n}(x)$ and a correlation matrix, $\mathbf{T}$ (a symmetric square matrix of order N). The output variable Z represents a transformed variable, and the task is to perform reliability analyses upon it. It is assumed that the analytical analysis of the transformation of input variables to Z is not possible due to the complexity of the computational model of $g(\mathbf{X})$. The failure probability is calculated as a probabilistic integral:

$$p_{\mathrm{f}} = P(Z \leq 0) = \int_{-\infty}^{\infty} I[g(\mathbf{X})] f_{\mathbf{X}}(\mathbf{x}) \mathrm{d}\mathbf{x} = \int_{D_{\mathrm{f}}} f_{\mathbf{X}}(\mathbf{x}) \mathrm{d}\mathbf{x}, \tag{2}$$

where $I[g(\mathbf{X})]$ is an indicator function that equals one for the failure event $(g(\mathbf{X}) \leq 0)$ and zero otherwise. In this way, the domain of integration of the joint probability distribution function $f_{\mathbf{X}}(\mathbf{x})$ is limited to the failure domain D_{f}, where $g(\mathbf{X}) \leq 0$. As mentioned in the introduction, explicit calculation of the integral in Eq. 2 is generally impossible, and in structural engineering practice, the

calculation of failure probability is solved using the aforementioned approximation methods. Their basic feature is an approximation, either of a limit state function or of a product of its evaluation: the safety margin Z (which is a random variable), see Fig. 1.

2.2 Response surface approximation

The general principle of the response surface method is to replace the original LSF with an approximated (simpler) function whose evaluation is not so time-consuming. The reliability indicator is then calculated using classical simulation methods but with the approximated function instead of the original one. Response surface methods provide a more accurate solution in comparison with FORM or SORM methods, where the limit state function is approximated by a linear or quadratic function at a design point. A second-order polynomial function is most often used in case of the polynomial RSM. Instead of replacing the original LSF with a polynomial one, it is also possible to use an approximation provided by an arbitrary surrogate model, or by an ANN, as is detailed in a later section of this paper. The ANN approximation function, when combined with classical simulation methods and applied to extensive reliability problems, is capable of ensuring the calculation of reliability indicators takes place in a reasonable time and with sufficient accuracy. The main advantage of the RSM is the reduction it permits in the number of calculations of the original function, and thus also the computational time, or the reduction in the variance of the obtained solutions with respect to the achieved accuracy.

Both methods, polynomial-based RSM and ANN-based RSM, are well described in previous work by the authors. For the sake of simplicity, only the most important points and equations are repeated in the following Sects. 2.2.1–2.2.2. For details, the reader is referred to [29].

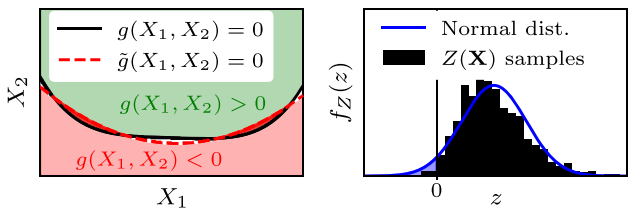

Fig. 1 Approximation of an original limit state function by a surrogate model (left), and approximation of the probability distribution of a safety margin by a suitable distribution based on goodness-of-fit tests (right)

2.2.1 Polynomial-based response surface approximation (POLY-RSM)

In general, a full second-order polynomial function [9] is most often employed. An iterative response surface approach based on a simplified polynomial function without mixed terms was presented in [10] in the form:

$$\tilde{g}(\mathbf{X}) = a + \sum_{i=1}^{n} b_i x_i + \sum_{i=1}^{n} c_i x_i^2, \tag{3}$$

where x_i, $i = 1, \ldots, n$ are the input basic variables and parameters a, b_i, c_i are the unknown regression coefficients of the approximation function that are obtained by conducting a series of numerical experiments with input variables selected according to an experimental design. Values of the interpolation points are situated around the mean values for the initial approximation. In the next step, the function $\tilde{g}(\mathbf{X})$ is used to obtain an estimate of the "design point", $\mathbf{X_D}$, for the surface $\tilde{g}(\mathbf{X}) = 0$ based on the assumption of uncorrelated Gaussian variables. Once $\mathbf{X_D}$ is found, $\tilde{g}(\mathbf{X_D})$ is evaluated and a new centre point for interpolation, $\mathbf{X_M}$, is chosen on a straight line from the mean vector $\overline{\mathbf{X}}$ to $\mathbf{X_D}$ in order to position the new centre point reasonably close to the exact limit state, i.e.:

$$\mathbf{X}_\mathrm{M} = \overline{\mathbf{X}} + (\mathbf{X}_\mathrm{D} - \overline{\mathbf{X}}) \frac{\tilde{g}(\overline{\mathbf{X}})}{\tilde{g}(\overline{\mathbf{X}}) - \tilde{g}(\mathbf{X}_\mathrm{D})}. \tag{4}$$

The same interpolation using Eq. 3 is repeated using $\mathbf{X_M}$ as the new anchor point, and hence, the total number of $g(\mathbf{X})$ evaluations (original LSF calculations) is $4n + 3$.

For the sake of completeness, the polynomial-based RSM appears to be sufficiently accurate when applied to reliability tasks, although several problems can arise. With an increasing number of input variables and thus a rise in the required accuracy of the approximation, the number of interpolation points also increases, which is a limiting factor in cases when the structural response is solved using time-consuming NLFEM analyses. Another issue, which is probably the largest problem, is the quality of the experimental design, i.e. the selection of interpolation points, as these have to be chosen so that the original function is best approximated around the design point. There are various methods of selecting interpolation points from the area around the limit state boundary, e.g. the gradient projection method [30] or the weight regression method [31, 32], in which higher values of weight coefficients are assigned to point around the design point when approximating the LSF. In connection with the location of interpolation points, it was further shown that the selection of points only from the tails of probability density functions of input variables does not lead to significant refinement in the quantification of the probability of failure [33], and finally, the proper

selection of interpolation points is also affected by the parameters of the LSF being approximated [34].

2.2.2 ANN-based response surface approximation (ANN-RSM)

An ANN-based response surface method is a signal processing system composed of simple processing elements, called artificial neurons, which are interconnected by direct links (weighted connections), see Fig. 2. The ANN serves as a surrogate model $\tilde{g}(\mathbf{X})$ for the approximation of an original $g(\mathbf{X})$, with $\mathbf{X}$ being the vector of input basic variables. The ANN has the ability to adapt itself by changing its connection strengths or structure, and hence, it is very efficient at fitting the LSF with only a small number of simulations. This number depends on several factors, such as the complexity of the original function, the number of input variables, their statistical correlation, and the quality of the sample set.

In the proposed method, a feed-forward multi-layer network type is used (e.g. [35–37]) with the artificial neurons organised into different layers – an input layer, several hidden layers, and an output layer. All of the neurons in a layer are connected to all of the neurons in the adjacent layers through unidirectional links represented by synaptic weights. These synaptic weights act as signal multipliers on the corresponding interconnections. Connections within a layer are not permitted (Fig. 2).

The input signal only moves in the forward direction, i.e. the data go from the input nodes through the hidden nodes (if any) to the output nodes. If the output vector of the whole neural network is required, output vectors have to be calculated layer by layer from the input layer to the output layer of the network. The output from a single neuron is calculated as (Fig. 2 right):

$$y = f(x) = f\left(\sum_{k} (w_k \cdot p_k + b)\right), \tag{5}$$

where k indicates the input number, w_k is the synaptic weight of the connecting path from the kth neuron of the previous layer, p_k is the input signal coming from the kth neuron of the previous layer, b is the bias of the neuron, and f is a transfer (activation) function of the neuron.

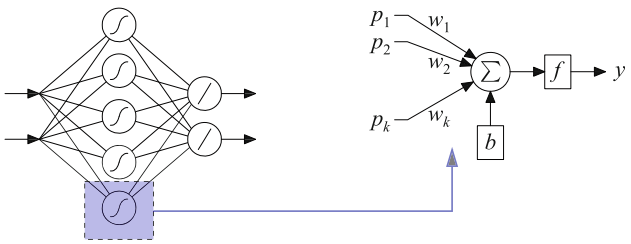

Fig. 2 Example of a feed-forward ANN (left) and a single neuron model (right)

ANNs must be trained (i.e. the values of synaptic weights and biases must be adjusted) to solve the particular problem for which they are intended. A feed-forward type network is trained using "supervised" learning, where a set of example pairs of inputs and corresponding outputs (p, y), $p \in \mathbf{P}$, $y \in \mathbf{Y}$ is introduced to the network. The aim of the subsequent optimisation procedure is to find a neural network function $f_{\text{ANN}} : \mathbf{P} \rightarrow \mathbf{Y}$ in the allowed class of functions that matches the examples. ANN training is an optimisation task which consists in minimising the criteria:

$$E = \frac{1}{2}\sum_{i=1}^{N}\sum_{k=1}^{K}\left(y_{ik}^{0} - y_{ik}^{*}\right)^2, \tag{6}$$

where N denotes the number of ordered input-output pairs in the training set, y_{ik}^{*} is the required new value of the kth output neuron at the ith input, and y_{ik}^{0} is the actual output value of the kth output neuron at this input. There are various optimisation methods by which the minimisation of criteria E is achieved, e.g. gradient descent methods, evolutionary methods, stochastic methods, or a combination of them.

The usefulness of the ANN model depends on both the size of the data, i.e. the number of features, and their corresponding distribution, as discussed in [38]. Since the number of computations of the nonlinear structural model may be limited due to the extreme computational demands, the efficiency of the ANN-RSM method is emphasized by using the small sample LHS simulation method, which is used for stochastic preparation of the training data set [29].

An important step before the training process begins is the design of the appropriate ANN structure, which is generally dependent on the type of reliability task. The number of inputs of the ANN, N_{inp}, is given by the number of input random variables, while the number of output neurons, N_{out}, corresponds to the LSF values (there is usually just one). Note that the number of "experimental samples" needed to adjust the parameters of the ANN-based response surface does not directly depend on the number of input random variables like it does in the case of a polynomial-based response surface approximation. Let us also mention that the number of inputs and the number of output neurons are known in advance. The number of hidden layers and the number of neurons in them are other parameters of the ANN. Two hidden layers with a sufficient number of neurons are enough to compute any reliability task. The best practice is to start with one hidden layer. If the neural network cannot be trained, then a second hidden layer is added.

A key influence on the complexity and performance of the ANN is also exerted by the choice of activation

function [39]. Depending on the type of original LSF being employed, both linear and nonlinear activation functions can be used. In general, if one wishes to introduce nonlinearity into the neural network, the nonlinear activation function must be employed. In that case, we use the hyperbolic tangent activation function, which was selected based on the initial tuning of the model hyperparameters.

2.3 The ANN-based inverse reliability method

Inverse reliability analysis can be categorised as a structural design, i.e. a means of identifying design parameters that enable the achievement of the desired reliability described by reliability indicators related to particular limit states. The parameters to be identified are deterministic or random design parameters related to the structure itself, the acting load or the surrounding environment. The known (in this case desired) response is a safety level described by reliability indicators. The functional relationship between design parameters and reliability indicators can take the form of an analytical formulation or a stochastic NLFEM model.

In addition to the vector of basic random variables $\mathbf{X} = X_1, X_2, \ldots, X_i, \ldots, X_n$, let us include the vector of design deterministic parameters $\mathbf{d} = d_1, d_2, \ldots, d_k, \ldots, d_p$ and the vector of the design parameters of random variables $\mathbf{r} = r_1, r_2, \ldots, r_l, \ldots, r_q$. Note that the design parameters of random variables can be statistical moments of the first and/or second order. In the case of multiple limit states, there are several safety margins Z_j and target failure probabilities $p_{f,j}$ or reliability indices β_j, where $j = 1, 2, \ldots, m$ is the number of limit state functions. The inverse problem can generally be stated as:

$$\begin{aligned} &\text{Given:} && p_{f,j} \text{ or } \beta_j \\ &\text{Find:} && \mathbf{d} \text{ and/or } \mathbf{r} \\ &\text{Subject to:} && Z_j = g(\mathbf{X}, \mathbf{d}, \mathbf{r})_j = 0 \text{ for } j = 1, 2, \ldots, m \end{aligned} \tag{7}$$

A soft computing-based inverse reliability method has been proposed by Lehký and Novák [28]. The method is based on the coupling of a stratified Latin hypercube sampling (LHS) simulation technique and an ANN. The ANN, as a cornerstone of the method, is used as a surrogate model of an unknown inverse function describing the relation between the design parameters and corresponding reliability indicators:

$$\mathbf{P} = f_{\text{ANN}}^{-1}(\mathbf{I}), \tag{8}$$

where: $\mathbf{P} = \mathbf{d} \cup \mathbf{r}$ is the vector of all design parameters (both deterministic and random; number of design parameters $u = p + q$), and $\mathbf{I} = \boldsymbol{\beta}$ (or $\mathbf{I} = \mathbf{p_f}$) is the vector of reliability indicators.

As mentioned above, the efficiency of the inverse method is emphasised by the utilisation of the small-sample LHS simulation method used for the stochastic preparation of the training set employed in training the ANN. For that purpose, the design parameters $\mathbf{P}$ (e.g. the mean values or standard deviations of selected random variables) are considered random variables with a scatter reflecting the physical range of design values. Subsequently, the calculation of reliability is performed using an appropriate simulation or approximation method, and reliability indicators $\mathbf{I}$ are obtained. Once the ANN has been trained, it represents an approximation which is subsequently used in the following way: to provide the best possible set of design parameters corresponding to the prescribed reliability. See [28] for a more complex explanation of the method.

The procedure of the ANN-based inverse reliability method is implemented as follows:

a. The design parameters are considered random variables with selected (physically reasonable) appropriate scatter and probability distribution. A rectangular distribution is often used.
b. Random samples of design parameters (possibly correlated) are generated using the LHS simulation method.
c. A stochastic model of the analysed problem is prepared including generated samples of design parameters.
d. Reliability analyses are performed repeatedly for individual samples of design parameters, and sets of reliability indicators, such as failure probabilities or reliability indices, are calculated.
e. Reliability indicators obtained from simulations are used together with the set of random design parameters as a training set for ANN training. During training, the discrepancy between the simulated and desired outputs of the ANN (here in the form of a mean square error according to Eq. 6) is minimised using an appropriate optimisation technique (e.g. back propagation methods, evolutionary algorithms).
f. Desired reliability indicators are used as an input signal which is distributed through the ANN structure to its output, where optimal design parameters are obtained.
g. Verification of the results via the calculation of failure probabilities related to limit state functions using the optimal parameters is carried out. Comparison with target failure probabilities will show the extent to which the inverse analysis was successful.

In the case of inverse reliability analysis, a double stochastic analysis is needed to prepare the training set for the ANN (steps b and d of the procedure). In the outer loop,

random realisations of design parameters are generated using the LHS simulation technique. The inner loop represents the reliability calculation for one particular realisation of design parameters. The number of simulations in the outer loop is driven by the ANN, and only a few dozen simulations are usually needed. The number of simulations in the inner loop depends on the utilised reliability method. When using the Monte Carlo method, as in the applications below, it is appropriate to run millions of simulations n_s. In this case, the failure probability is calculated as

$$p_f = \int_{-\infty}^{\infty} I[\tilde{g}(\mathbf{X})] f_{\mathbf{X}}(\mathbf{x}) \mathrm{d}\mathbf{x} = \lim_{n_s \to \infty} \frac{1}{n_s} \sum_{j=1}^{n_s} I[\tilde{g}(\mathbf{X})]. \quad (9)$$

2.4 The inverse response surface method

As described in Sect. 2.2, the response surface approximation is an alternative to the real LSF. However, in contrast to the forward approach, when a structure is being designed, the function values that are used to construct the response surface are not available until the desired design variables have been determined. Therefore, an inverse response surface method (IRSM) is proposed.

This IRSM method is based on a coupling of the adaptive response surface method developed by Bucher and Bourgund [10] and the ANN-based inverse reliability method created by Lehký and Novák [28] (see also Sect. 2.3). The method is inspired by the procedure laid out by Li [40], which combines the response surface method with the Newton-Raphson iterative algorithm to solve an inverse reliability problem [22]. The method proposed in this paper utilises ANN and LHS methods, which makes it more robust and efficient, and therefore feasible for use when solving time-consuming problems such as structural design.

An iterative scheme to upgrade the response surface model and, at the same time, to accomplish inverse reliability analysis is proposed as follows:

1. In the first step of the IRSM, the initial values for the design parameters are used to construct the initial response surface using a direct RSM (polynomial-based or ANN-based methods are used in this paper; see Sect. 2.2). Based on this approximate response surface (see the light orange dashed line in Fig. 3b), ANN-based inverse reliability analysis is carried out, and a new estimate of design parameters is obtained as well as the design point. A response surface with the newly estimated design parameters is depicted using a dark orange solid line in Fig. 3b. Note here that in the proposed small-sample polynomial- or ANN-based RSM, the LHS method is not utilised for the evaluation of the reliability indicators (failure probabilities or reliability indices), but it is employed for the efficient stochastic preparation of the training set for ANN training. The reliability indicators are calculated using classical simulation or approximation methods (e.g. the Monte Carlo method, FORM, etc.).
2. In the next step, the new anchor point is calculated from the design point using Eq. 4. The obtained anchor point is used as a new centre point and employed together with the previously obtained design parameters when preparing a new set of samples for the construction of an updated response surface (see the brown dashed line in Fig. 3c). At first glance, this updated response surface may appear worse than the original response surface (dark orange solid line). However, on looking more closely, it is clear that there has been a significant refinement of the approximation, particularly in the failure region where $g(\mathbf{X}, \mathbf{P}) < 0$. Moreover, the determined design parameters were obtained with the initial (inaccurate) response surface.
3. Based on this updated response surface, ANN-based inverse reliability analysis is carried out again to seek a new set of design parameters and a new design point. The updated response surface together with the updated estimate of design parameters is depicted by a red solid line in Fig. 3d.
4. Finally, the process is repeated until convergence is achieved at design parameters with acceptable tolerance.

The individual steps of the proposed procedure are schematically shown in Fig. 3a.

3 Numerical examples

Three different examples were selected to show the procedure of the proposed IRSM. An explicit nonlinear function with only one design parameter to be identified is described in Sect. 3.1. Here, the whole IRSM process is described in detail. Sect. 3.2 focuses on an example in which the dimensions of a timber beam are to be designed, requiring the identification of two parameters for two limit states. A post-tensioned bridge made of MPD girders is the subject of the last example (Sect. 3.3). In this case, the limit state function is given in implicit form as an NLFEM model. The decompression and crack initiation limit states for the target bridge load-bearing capacity are solved to determine the values of two bridge design parameters. The accuracy of the response surfaces and surrogate models used for the inverse reliability problems is discussed in terms of an absolute percentage error (APE) and a coefficient of determination (R^2). These metrics are defined in the form of:

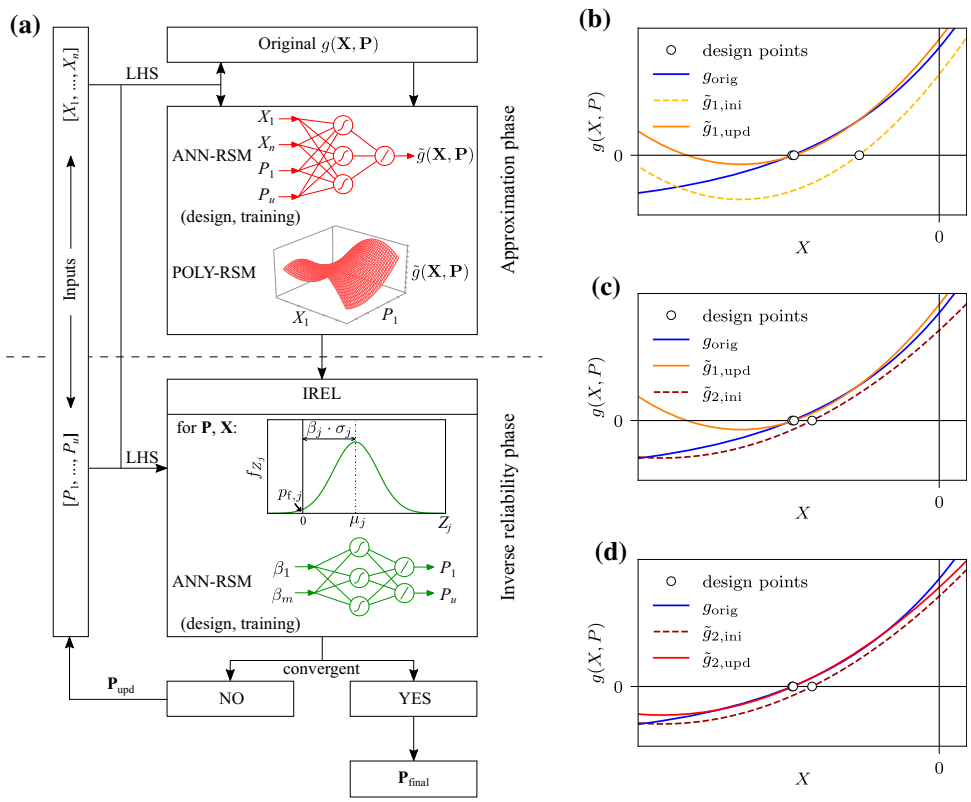

Fig. 3 Schematic diagram of the proposed inverse response surface method: **a** iterative procedure; **b** response surface with initial estimate of design parameters; **c** updated response surface; **d** final response surface achieved with acceptable tolerance

$$\mathrm{APE} = 100 \cdot \frac{|V_\mathrm{t} - V_\mathrm{a}|}{V_\mathrm{t}}, \tag{10}$$

$$R^2 = 1 - \frac{(V_\mathrm{t} - V_\mathrm{a})^2}{V_\mathrm{t}^2}, \tag{11}$$

where V_t is the target value and V_a is the approximated value.

Table 1 Stochastic model for the example with explicit LSF

Variable	Distribution	Mean value	Standard deviation
X_1	Normal	0	1
X_2	Normal	0	1
d	Deterministic	?	–

3.1 An explicit nonlinear limit state function

An explicit nonlinear LSF was selected to show the proposed IRSM procedure in detail. The function was adopted from [30] and was defined as:

$$g(\mathbf{X}) = \exp[0.4(X_1 + 2) + 6.2] - \exp(0.3X_2 + d) - 200, \tag{12}$$

where X_1 and X_2 were the standard normal variables, and d was an unknown deterministic design parameter subjected to identification (marked with "?" in Table 1); see the stochastic model in Table 1. The target reliability index was considered to be $\beta = 2.688$, which corresponds to the target value of $d = 5$ (calculated using 10 million Monte Carlo simulations of the original LSF).

In order to construct the response surface and perform an ANN-based inverse reliability analysis (Fig. 3a), the design parameter d has been treated as a uniformly distributed random variable. Two cases with the initial range of values were used; see Table 2. In case 1, a wider range of values was used with the target value of parameter d inside this range, i.e. $d \in \langle 4; 8 \rangle$. In case 2, the target value of parameter d was placed outside of a narrower range of values, i.e. $d \in \langle 6; 8 \rangle$.

Both polynomial-based and ANN-based response surface approximations (see the approximation phase in Fig. 3a) were used as substitutes for the original LSF in Eq. 12. A two-degree polynomial response surface without the mixed terms employed in Eq. 3 has been used in the case of the POLY-RSM. In the case of the ANN-RSM, an ANN with three input neurons corresponding to variables X_1 and X_2, and design parameter d, one linear output neuron corresponding to the value of the original LSF $g(\mathbf{X})$ and eight nonlinear neurons in a hidden layer has been used as a substitute for the original LSF; see Fig. 4 (left). A hyperbolic tangent activation function in the hidden layer and a linear activation function in the output layer were

Table 2 Randomisation of the design parameter for the example with explicit LSF

Variable	Distribution	Mean value	Standard deviation (COV)	Min	Max
d – case 1	Rectangular	6	1.155 (0.19)	4	8
d – case 2	Rectangular	7	0.577 (0.08)	6	8

used. In order to calculate unknown coefficients of the polynomial response surface, 30 evaluations of the original LSF $g(\mathbf{X})$ were carried out with random samples of input parameters generated via the LHS method according to the stochastic model (see Tables 1 and 2). The same 30 random samples of input parameters generated via the LHS method were used as the training set for the ANN training, which was performed using the gradient descent method with momentum. The learning rate was 0.01, and the momentum was 0.5.

An ANN-based inverse reliability analysis (see the inverse reliability phase in Fig. 3a) was carried out using the created response surfaces. The utilised ANN consisted of one input to the network corresponding to reliability index β, two nonlinear neurons in a hidden layer and a linear output neuron corresponding to the design parameter d; see Fig. 4 (right). A hyperbolic tangent activation function in the hidden layer and a linear activation function in the output layer were used again. In order to create the training set, reliability calculations using 1 million Monte Carlo simulations were performed for each of the 30 individual random samples of design parameter d. Thus, the vector $\boldsymbol{\beta}$ of the reliability indices was obtained. After the ANN had been trained, it was ready to provide the best design parameter related to the initial response surface. This was performed by means of a network simulation using target reliability index $\beta = 2.688$ as an input.

Finally, the reliability level was calculated with the identified design parameter and compared to the target value in order to verify the accuracy achieved in the identification process.

To achieve a good level of accuracy, the response surface was subsequently updated based on an iterative solution. The value of design parameter d obtained in the calculation was used in the construction of an updated response surface for the next iteration. Here, the stochastic model was changed with respect to the updated design parameter and the new anchor point calculated according to Eq. 4, i.e. random sampling was performed in a region closer to the failure domain. The standard deviation of the design parameter has been reduced to half of the original value in order to speed up the process and improve its convergence.

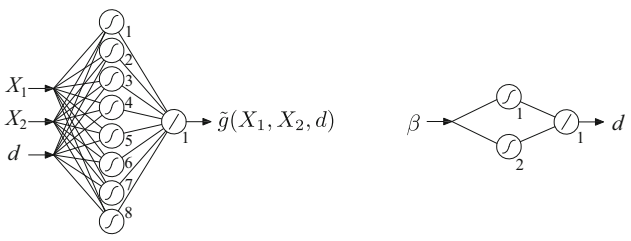

Fig. 4 Schematic view of the ANN utilised to create the ANN-based response surface (left) and the ANN for the inverse reliability analysis (right)

Table 3 summarises the design parameter and reliability index values during the iteration process. Note that reliability index β was calculated by 10 million Monte Carlo simulations of the response surface. The whole process of the IRSM was repeated until the desired accuracy was reached. In this example, 2 or 3 iterations were sufficient to reach the acceptable accuracy.

Analysis of the results for case 1 (with a wide initial range of design parameter values) shows that both approximations were able to find the target design parameter value in two iterations. The ANN-RSM method had negligibly better accuracy. A graphical comparison is shown in Fig. 5. Case 2 (where the target value of the design parameter was placed outside of a narrower range of values) proved to be slightly more difficult and sensitive to the surrogate model used. The ANN-RSM needed 3 iterations to identify the target value of the design parameter. In contrast, the POLY-RSM did not reach the correct result. This was due to its insufficiently accurate approximation of the response surface for the initial estimation of the design parameter. This led to inaccurate estimation both of the design point and of the value of the updated design parameter. The obtained updated response surface did not allow the detection of any failures or the estimation of the design parameter (N/A values in the Table 3). The same finding was obtained using a polynomial response surface with mixed terms.

Figure 5 shows how polynomial-based and ANN-based response surfaces approach the real LSF (g_{orig}, blue coloured surface) for case 1 of the example. In the figure, there are response surfaces ($\tilde{g}_{i,v}$, red coloured surfaces) corresponding with individual iterations of the process ($i = 1$ and 2 in this case), each depicted for both the initial value ($v =$ "ini") as well as the updated value ($v =$ "upd") of the design parameter. The grey coloured surface corresponds to the failure boundary $g(\mathbf{X}) = 0$ and splits the space into a safe domain ($g(\mathbf{X}) > 0$) and a failure domain ($g(\mathbf{X}) < 0$). Note that in order to improve the visibility of the failure domain, the graph has a flipped vertical axis, i.e. negative values of $g(\mathbf{X})$ are above the failure boundary.

Table 3 Results of the iterative process for the example with explicit LSF

	Parameter	Identification			Target value
		iteration 1 (APE; R^2)	iteration 2 (APE; R^2)	iteration 3 (APE; R^2)	
POLY-RSM:	d – case 1	4.8321	4.9996	–	5.000
		(3.36; 0.9989)	(0.01; 1.0000)	(–)	
	β – case 1	2.979	2.669	–	2.688
		(10.86; 0.9882)	(0.68; 1.0000)	(–)	
	d – case 2	4.4803	N/A	–	5.000
		(10.39; 0.9892)	(–)	(–)	
	β – case 2	−0.387	N/A	–	2.688
		(114.41; −0.3089)	(–)	(–)	
ANN-RSM:	d – case 1	5.0512	4.9999	–	5.000
		(1.02; 0.9999)	(0.00; 1.0000)	(–)	
	β – case 1	2.690	2.685	–	2.688
		(0.11; 1.0000)	(0.10; 1.0000)	(–)	
	d – case 2	5.5894	4.9369	4.9906	5.000
		(11.79; 0.9861)	(1.26; 0.9998)	(0.19; 1.0000)	
	β – case 2	2.299	2.655	2.686	2.688
		(14.45; 0.9791)	(1.20; 0.9999)	(0.07; 1.0000)	

The blue and black lines represent the intersections of the original and approximated functions, respectively, with the "zero surface".

It is obvious that the POLY-RSM matches the entire surface of the original LSF reasonably well in all steps of the iterative process. In contrast, the ANN-RSM progressively refines the approximation mainly in the failure domain, which is, however, essential for the determination of the reliability indicator. The ANN-RSM thus proved its robustness and suitability for reliability-based design.

3.2 A timber beam

In this example, two design parameters corresponding to mean values of width, b, and height, h, as cross-sectional dimensions of a simply supported timber beam were to be identified using the proposed IRSM in order to fulfil the target reliability levels for the ultimate and serviceability limit state.

The ultimate limit state (ULS) was defined according to the LSF in the form of:

$$g_{\mathrm{ULS}} = M_{\mathrm{Rd}} - M_{\mathrm{Ed}} = \Phi_{\mathrm{R}} \frac{1}{6} b h^2 k_{\mathrm{mod}} f_{\mathrm{m}} - \Phi_{\mathrm{E}} \frac{1}{8} (g+q) l^2. \tag{13}$$

The target reliability index value was set up as $\beta_{\mathrm{ULS}} = 3.8$. In the case of the serviceability limit state (SLS), the limit value of the midspan deflection was analysed and the LSF was evaluated according to:

$$g_{\mathrm{SLS}} = u_{\mathrm{lim,fin}} - u_{\mathrm{net,fin}} = = \frac{l}{200} - \Phi_{\mathrm{E}} \frac{5}{384} \frac{l^4}{E \frac{1}{12} b h^3} [g(1+k_{1,\mathrm{def}}) + q(1+k_{2,\mathrm{def}})], \tag{14}$$

with the target value of reliability index $\beta_{\mathrm{SLS}} = 1.5$. The meaning of the input variables for the LSFs mentioned above was as follows: l was the span of the beam, b and h were the width and height of the beam (subjects of identification marked with "?" in Table 4), E was the modulus of elasticity, f_{m} was the flexural strength of the timber, g and q were the dead-load and payload of the beam, Φ_{R} and Φ_{E} were the model uncertainties of the response and action, and k_{mod}, $k_{1,\mathrm{def}}$ and $k_{2,\mathrm{def}}$ were the modification and creep coefficients of the timber, these being $k_{\mathrm{mod}} = 0.8$, $k_{1,\mathrm{def}} = 0.8$ and $k_{2,\mathrm{def}} = 0.25$. For the stochastic model of the input variables see Table 4.

In the first step of the IRSM procedure, the design parameters mean b and mean h were treated as uniformly distributed random variables; see Table 5. ANN-based response surface approximations were used to substitute the original LSFs in Eqs. 13–14. ANNs with six or seven input neurons based on the LSF, one linear output neuron and five nonlinear neurons in a hidden layer were used. 50 random samples of input parameters generated by the LHS method were employed to set the response surfaces. The gradient descent method with momentum was used to train the ANNs. The learning rate was between −0.001 and 0.01, and the momentum was 0.5.

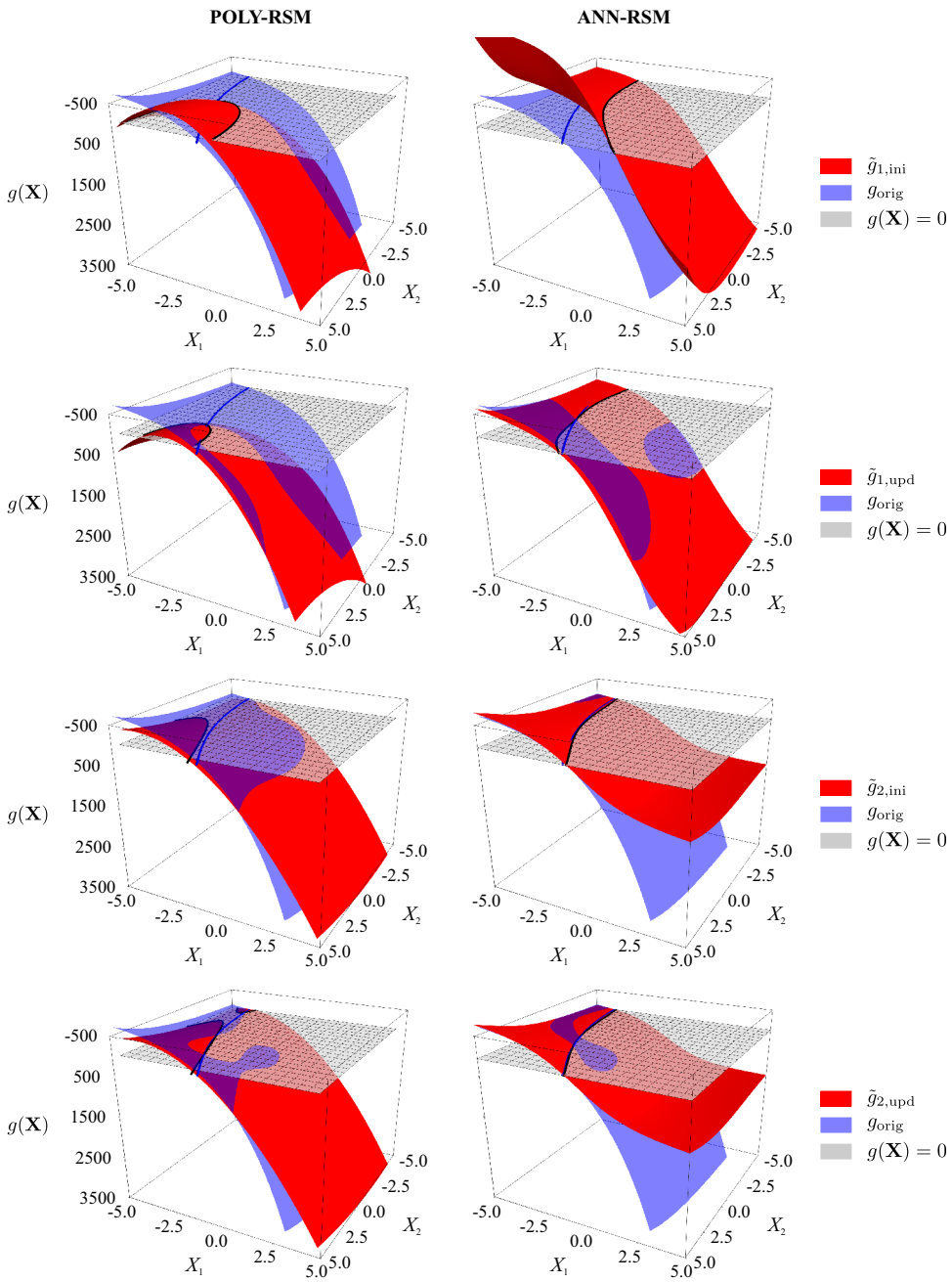

Fig. 5 Evolution of response surfaces (case 1 of Example 1) in an iterative process: POLY-RSM (left), and ANN-RSM (right)

The ANN-based inverse reliability analysis was carried out using the constructed response surfaces. The utilised ANN consisted of two inputs to the network corresponding to reliability indices β_{ULS} and β_{SLS}, five nonlinear neurons in a hidden layer and two linear output neurons corresponding to the identified design parameters mean b and mean h. The training set was created using 50 LHS random simulations of the design parameters. Reliability indicators in the form of reliability indices for the SLS and ULS were assessed based on the FORM method in this case. The results of the iterative IRSM process are summarised in Table 6. In this example, 4 iterations were performed to show gradual convergence of the design parameters. Note that from a practical point of view, two iterations would be sufficient to obtain design parameters with acceptable accuracy. The target values in Table 6 were obtained using 100 million Monte Carlo simulations since the LSFs in this test example were explicitly defined functions whose evaluation was relatively fast. Note that a hyperbolic tangent activation function in the hidden layer and a linear activation function in the output layer were used during the ANN training process.

Table 4 Stochastic model for the example of a timber beam

Variable	Distribution	Mean value	Standard deviation (COV)
l [m]	Deterministic	3.5	–
b [m]	Normal	?	? (0.05)
h [m]	Normal	?	? (0.05)
E [GPa]	Log-normal (2par.)	10	1.3 (0.13)
f_m [MPa]	Log-normal (2par.)	34	8.5 (0.25)
g [kN/m]	Gumbel Max EV I	1.686	0.1686 (0.10)
q [kN/m]	Gumbel Max EV I	2.565	0.7695 (0.30)
Φ_R [–]	Log-normal (2par.)	1	0.1 (0.10)
Φ_E [–]	Log-normal (2par.)	1	0.1 (0.10)

Table 5 Randomisation of the design parameters for the example of a timber beam

Variable	Distribution	Mean value	Standard deviation (COV)	Min	Max
mean b	Rectangular	0.10	0.014434 (0.14)	0.11	0.15
mean h	Rectangular	0.25	0.014434 (0.06)	0.20	0.25

Table 6 Results of the iterative process for the example of a timber beam

Parameter	Identification				Target value
	iteration 1 (APE; R^2)	iteration 2 (APE; R^2)	iteration 3 (APE; R^2)	iteration 4 (APE; R^2)	
mean b	0.1187	0.1239	0.1268	0.1288	0.1285
	(7.62; 0.9942)	(3.53; 0.9988)	(1.26; 0.9998)	(0.25; 1.0000)	
mean h	0.2181	0.2152	0.2131	0.2126	0.2127
	(2.52; 0.9994)	(1.17; 0.9999)	(0.20; 1.0000)	(0.06; 1.0000)	
β_{ULS}	3.7899	3.8047	3.7993	3.8012	3.8
	(0.27; 1.0000)	(0.12; 1.0000)	(0.02; 1.0000)	(0.03; 1.0000)	
β_{SLS}	1.4986	1.4933	1.4971	1.5047	1.5
	(0.09; 1.0000)	(0.45; 1.0000)	(0.19; 1.0000)	(0.31; 1.0000)	

3.3 A post-tensioned composite bridge made of MPD type girders

A single-span post-tensioned concrete bridge built in 1957 in the Czech Republic was chosen as an example to illustrate the utilisation of the IRSM in the case of NLFEM analysis (Fig. 6). This example follows on from a work by the authors [29] in which the small-sample response surface method was used to approximate an original LSF in order to reduce the computational effort in the case of time-consuming FEM analyses of structures.

The analysed bridge is made of twelve precast post-tensioned concrete MPD3 (outer) and MPD4 (intermediate) type girders. Each of the MPD girders was composed of six segments that are connected to each other by transverse joints; see Fig. 6 top right. In order to model the structural response, a simplified numerical FEM model was created in ATENA 2D software [41]. Here, data on the geometry and material parameters assessed within the bridge diagnostic survey were used. The following load cases were modelled: the dead load of the structure, longitudinal prestressing, secondary dead load and traffic load corresponding to the normal loading class according to Czech technical standard ČSN 73 6222 [42].

Based on the former sensitivity analysis of the input variables, the reduced stochastic model (Table 7) was used, within which only the most significant variables affecting the structural response were randomised. These were the tensile strength, f_t, and fracture energy, G_f, of the concrete of the transverse joints, the prestressing force in the bottom tendon, P_1, and the secondary dead load, $g_{1,n}$. The statistical correlation between the tensile strength and fracture energy of the concrete was also considered and imposed using a simulated annealing approach [43]. The value $\rho(f_t, P_1) = 0.8$ was defined with respect to previously performed tests [44].

There was high variability in the compressive strength values measured for the concrete of the joints between

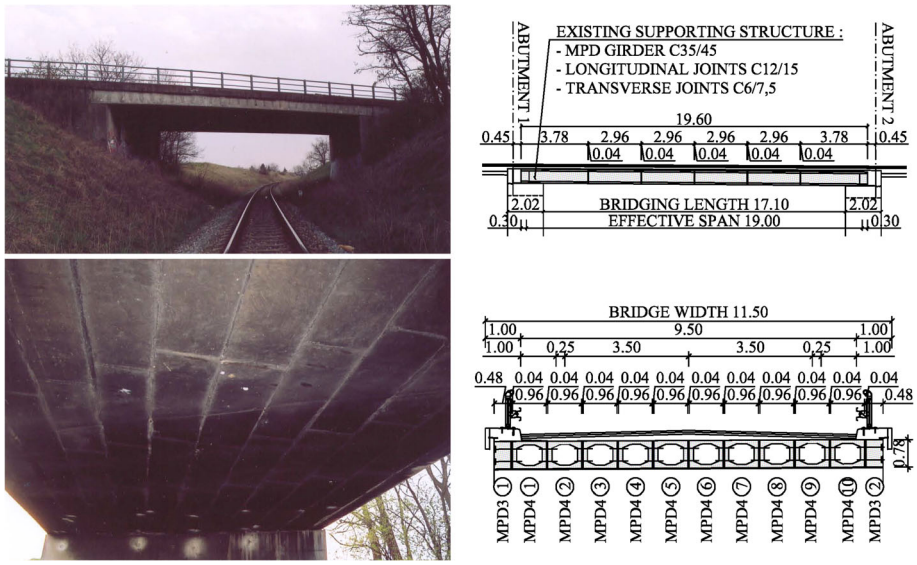

Fig. 6 Side and bottom view (left) and longitudinal and transversal section (right) of the analysed bridge

Table 7 Stochastic model for the example of a bridge made of MPD girders

Variable	Distribution	Mean value	Standard deviation (COV)
f_t [MPa]	Weibull min (2par.)	?	? (0.35)
G_f [N/m]	Weibull min (2par.)	47.82	11.955 (0.25)
P_1 [MN]	Normal	?	? (0.09)
$g_{1,n}$ [kN/m]	Normal	65.55	3.2775 (0.05)

precast segments of the bridge, which was probably caused by the spatial deterioration of the bridge and accompanying uncertainty in the current loss of prestressing. As a result, the mean values of parameters f_t and P_1 were considered as uncertain design parameters (marked with "?" in Table 7) with the aim of finding their critical values corresponding to the desired reliability level and load-bearing capacity. According to the diagnostic survey and the needs of the bridge administrator, the desired load-bearing capacity related to the normal loading class was considered to be 25 tons.

Only serviceability limit states were investigated as being critical for the assessment of the load-bearing capacity of the bridge. Two limit states were taken into account – the serviceability limit state of decompression (SLSD) and the serviceability limit state of crack initiation (SLSC). Both limit states had an implicit form, i.e. structural resistance was calculated using the NLFEM model. The target reliability indices were considered to be $\beta_{SLSD} = 0$ and $\beta_{SLSC} = 1.3$, respectively.

In order to construct the response surface and perform ANN-based inverse reliability analysis, the identified design parameters mean f_t and mean P_1 were randomised with initial ranges according to Table 8. ANN-based response surface approximations were created as substitutes for the original LSFs corresponding to both analysed limit states. The ANNs consisted of four inputs to the network corresponding to four input random variables according to the stochastic model in Table 7, three nonlinear neurons in a hidden layer and a linear output neuron corresponding to the safety margin of the particular limit state. 50 random samples of input parameters generated by the LHS method were used to set the response surfaces. The gradient descent method with momentum was used to train the ANNs as in the previous examples. The learning rate was between −0.001 and 0.01, and the momentum was 0.5.

The inverse reliability analyses were carried out based on the constructed response surfaces. The ANN utilised in the inverse reliability analyses consisted of two inputs to the network corresponding to the reliability indices of two analysed limit states, five nonlinear neurons in a hidden layer and two linear output neurons corresponding to the mean values of two design parameters, mean f_t and mean P_1. In order to create the ANN training set, reliability calculations using a hundred thousand Monte Carlo simulations were performed with 50 individual vectors of random samples of the design parameters. A hyperbolic tangent activation function in the hidden layer and a linear

Table 8 Randomisation of the design parameters for the example of a bridge made of MPD girders

Variable	Distribution	Mean value	Standard deviation (COV)	Min	Max
mean f_t	Rectangular	2.4	0.346 (0.14)	1.8	3.0
mean P_1	Rectangular	15	1.732 (0.12)	12	18

activation function in the output layer were used as in the previous examples during the ANN training process.

An iterative IRSM process was carried out with updated design parameters. Here, the stochastic model was changed with respect to the updated design parameters and the new anchor points calculated according to Eq. 4. Table 9 shows the values obtained for the design parameters and reliability indices during the iteration process. Here, 2 iterations were enough to reach acceptable accuracy. Note that the reliability indices were calculated via a hundred thousand Monte Carlo simulations of response surfaces. The target values of the design parameters are not known in this example, as it takes anything from tens of minutes to an hour to quantify the original LSF in the form of an NLFEM model, and so performing this many simulations is not practically possible. This is a typical example of a case where the use of a response surface is necessary.

The results of the iterative process in Table 9 show a more stable convergence when identifying the prestressing force compared to the tensile strength of concrete. This is in agreement with the findings of the sensitivity analysis, which confirmed the dominant influence of the prestressing on response in both the SLSD and the SLSC, while tensile strength is important just for the SLSC. The results also show that the required mean value of concrete tensile strength in transverse joints corresponds to concrete strength class C20/25. It matches the concrete type used for transverse joints during bridge construction, as was also confirmed by the findings of the diagnostic survey. Note that the requirement for reliability index $\beta_{SLSC} = 1.3$ in the case of the SLSC is relatively strict too. For lower values, an even lower demand for concrete strength would be obtained. The resulting requirement for the value of prestressing force is almost the same as that estimated according to code specifications, where loss of prestressing was considered to be 17 %. The identified prestressing force value indicates a loss of prestressing equal to 15 %. From both results we can conclude that the requirement for a normal load-bearing capacity of $V_n = 25$ t is adequate, and the desired level of safety would be met.

Table 9 Results of the iterative process for the example of a bridge made of MPD girders

Parameter	Identification		Target value
	iteration 1 (APE; R^2)	iteration 2 (APE; R^2)	
mean f_t	2.916	2.277	–
mean P_1	14.538	14.544	–
β_{SLSD}	0.076 (0.0758*)	0.005 (0.0050*)	0.000
β_{SLSC}	1.384 (6.45; 0.9958)	1.310 (0.79; 0.9999)	1.300

*Given a zero target value, the absolute error $AE = |V_t - V_a|$ is evaluated in this case

4 Discussion and conclusion

The paper presents an adaptive ANN-based inverse response surface method. This approach effectively combines the adaptive response surface method with ANN-based inverse reliability analysis. From the described theory and the results of application examples, the following conclusions can be drawn:

- Employing the response surface method in solving the inverse reliability problem can lead to inaccurate estimates of design parameters due to initial uncertainties in their true values which result in an inaccurate initial approximation of the original limit state function. This is obvious from the results of the example in Sect. 3.1. For the case with the target value of the identified parameter inside the initial range of values, the surrogate models provided very accurate results. When estimating the design parameter d, the APE was equal to 3.36 % and 1.02 % for the POLY-RSM and ANN-RSM in the first iteration, respectively. After the second iteration, the APE decreased to 0.01 % and 0.00 %, respectively. For the case with the target value of the parameter outside the initial range of values, the APE for POLY-RSM was equal to 10.39 % after the first iteration. After the second iteration, the POLY-RSM did not achieve the correct result. In the case of ANN-RSM, three iterations were required to identify the value of the design parameter with the APE equal to 11.79 %, 1.26 % and 0.19 %, respectively.
- In order to obtain correct values for the design parameters, it is necessary to iteratively refine their

estimates, which goes hand in hand with a gradual refinement of the response surface in the failure region.

- The ANN-based inverse reliability method is used within the proposed inverse response surface method to identify design parameters, where the ANN represents a surrogate model of the inverse relationship between design parameters and reliability indicators. This makes the determination of the resulting design parameters very fast, and the values obtained implicitly guarantee the desired reliability. Using the ANN-RSM, the reliability indices β were evaluated with very low APE values in all the examples and iterations. In the case of the explicit form of the LSF (example in Sect. 3.2), the APE values were up to 0.50 % in all iterations. The efficiency of the proposed method was also proved in the case of the LSF specified in the implicit form as the NLFEM model (Sect. 3.3). Here, the APE was equal to 6.45 % after the first iteration and 0.79 % after the second iteration. Compared to POLY-RSM, the ANN-RSM was able to achieve the target reliability index value even when the target value of the identified parameter was outside the initial range of values (Sect. 3.1). The APE value was 14.45 % after the first iteration and 0.07 % after the last iteration. (In this case, three iterations were needed.)
- An important step in the whole procedure is to choose a good surrogate model to approximate the limit state function. In practical cases, it always depends on the type of problem to be solved. In the examples, we have presented, in the cases with nonlinear LSF, the ANN response surface was confirmed to be more efficient compared to the polynomial response surface, which is consistent with our earlier findings.
- The number of iterations of the adaptive process depends on the type of problem being solved, the surrogate model used and the initial estimation of the design parameters. In practical applications, it will always depend on the time required to evaluate the original model. In extreme cases, e.g. when analysing large structures using the NLFEM, just one level of refinement often yields a significant qualitative improvement in the estimation of design parameters compared to the initial response surface estimate. In extreme cases, it is always necessary to consider whether adding another iteration, which means running dozens of simulations that may each take several hours, is worth it for the slight refinement of the results that may occur. In example 3.3, the absolute percentage error for SLSC decreased from 6.45 % to 0.79 % after the second iteration, and for SLSD, the absolute error of the reliability index value decreased from 0.0758 to 0.0050.

The presented inverse response method, thanks to its advantageous synergy of traditional and modern mathematical methods based on artificial intelligence, brings reliability-based design and optimisation into common engineering practice while maintaining sufficient accuracy and acceptable time demands.

Acknowledgements This work was supported by project No. 20-01734S awarded by the Czech Science Foundation (GACR).

Declaration

Conflict of interest The authors declare that they have no conflict of interest.

References

1. Hammersley JM, Handscomb DC (1964) Monte Carlo methods. Methuen, London, Wiley, New York
2. McKay MD, Conover WJ, Beckman RJ (1979) A comparison of three methods for selecting values of input variables in the analysis of output from a computer code. Technometrics 21:239–245
3. Lehký D, Slowik O, Novák D (2018) Reliability-based design: artificial neural networks and double-loop reliability-based optimization approaches. Adv Eng Softw 117:123–135
4. Kala Z (2020) Sensitivity analysis in probabilistic structural design: a comparison of selected techniques. Sustainability 12(11):4788
5. Hasofer AM, Lind NC (1974) Exact and invariant second-moment code format. J Eng Mech Div 100(1):111–121
6. Fiessler B, Neumann H-J, Rackwitz R (1979) Quadratic limit states in structural reliability. J Eng Mech ASCE 105(4):661–676
7. Box GEP, Wilson KB (1951) On the experimental attainment of optimum conditions. J R Stat Soc Ser B 13(1):1–45
8. Myers RH (1971) Response Surface Methodology. Allyn and Bacon, New York
9. Bucher CG, Chen YM, Schuëller GI (1989) Time variant reliability analysis utilizing response surface approach. In: Thoft-Christensen P (ed) Reliability and optimization of structural systems, vol 48. Springer, Berlin, pp 1–14
10. Bucher CG, Bourgund U (1990) A fast and efficient response surface approach for structural reliability problems. Struct Saf 7(1):57–66. https://doi.org/10.1016/0167-4730(90)90012-E
11. Ghanem RG, Spanos PD (1991) Stochastic finite elements: a spectral approach. Springer, Berlin
12. Hurtado JE (2004) An examination of methods for approximating implicit limit state functions from the viewpoint of statistical learning theory. Struct Saf 26(3):271–293
13. Kaymaz I (2005) Application of Kriging method to structural reliability problems. Struct Saf 27(2):133–151
14. Echard B, Gayton N, Lemaire M (2011) AK-MCS: an active learning reliability method combining Kriging and Monte Carlo simulation. Struct Saf 33(2):145–154
15. Echard B, Gayton N, Lemaire M, Relun N (2013) A combined importance sampling and Kriging reliability method for small failure probabilities with time-demanding numerical models. Reliab Eng Syst Saf 111:232–240
16. Aydın S (2021) Cross-validated adaboost classification of emotion regulation strategies identified by spectral coherence in resting-state. Neuroinformatics. https://doi.org/10.1007/s12021-021-09542-7

17. Taherkhani A, Cosma G, McGinnity TM (2020) AdaBoost-CNN: an adaptive boosting algorithm for convolutional neural networks to classify multi-class imbalanced datasets using transfer learning. Neurocomputing 404:351–366
18. Aydın S (2020) Deep learning classification of neuro-emotional phase domain complexity levels induced by affective video film clips. IEEE J Biomed Health Inf 24(6):1695–1702. https://doi.org/10.1109/JBHI.2019.2959843
19. Winterstein SR, Ude TC, Cornell CA (1994) Environmental parameters for extreme response: inverse form with omission factors. In: Schuëller, Shinozuka and Yao (Eds.), Proceedings of ICOSSAR'93: structural safety and reliability, Innsbruck, Austria, pp. 551–557, Rotterdam: Balkema
20. Maes MA, Huyse L (1997) Developing structural design criteria with specified response reliability. Can J Civ Eng 24(2):201–210
21. Der Kiureghian A, Zhang Y, Li CC (1994) Inverse reliability problem. J Eng Mech 120(5):1154–1159
22. Li H, Foschi RO (1998) An inverse reliability method and its application. Struct Saf 20:257–270
23. Sadovský Z (2000) Discussion on: an inverse reliability method and its application. Struct Saf 22(1):97–102
24. Mínguez R, Castillo E, Hadi AS (2005) Solving the inverse reliability problem using decomposition techniques. Struct Saf 27:1–23
25. Shayanfar MA, Massah SR, Rahami H (2007) An inverse reliability method using networks and genetic algorithms. World Appl Sci J 2(6):594–601
26. Cheng J, Li QS (2009) Application of the response surface methods to solve inverse reliability problems with implicit response functions. Comput Mech 43(4):451–459
27. António C, Hoffbauer L (2010) Uncertainty propagation in inverse reliability-based design of composite structures. Int J Mech Mater Des 6(1):89–102
28. Lehký D, Novák D (2012) Solving inverse structural reliability problem using artificial neural networks and small-sample simulation. Adv Struct Eng 15(11):1911–1920
29. Lehký D, Šomodíková M (2017) Reliability calculation of time-consuming problems using a small-sample artificial neural network-based response surface method. Neural Comput Appl 28(6):1249–1263
30. Kim S-H, Na S-W (1997) Response surface method using vector projected sampling points. Struct Saf 19(1):3–19. https://doi.org/10.1016/S0167-4730(96)00037-9
31. Kaymaz I, McMahon CA (2005) A response surface method based on weighted regression for structural reliability analysis. Probab Eng Mech 20(1):11–17. https://doi.org/10.1016/j.probengmech.2004.05.005
32. Eshghi AT, Lee S (2019) Adaptive improved response surface method for reliability-based design optimization. Eng Opt 51(12):2011–2029
33. Rajashekhar MR, Ellingwood BR (1993) A new look at the response surface approach for reliability analysis. Struct Saf 12(3):205–220. https://doi.org/10.1016/0167-4730(93)90003-J
34. Guan XL, Melchers RE (2001) Effect of response surface parameter variation on structural reliability estimates. Struct Saf 23(4):429–444. https://doi.org/10.1016/S0167-4730(02)00013-9
35. Cichocki A, Unbehauen R (1993) Neural networks for optimization and signal processing. Wiley, Teubner, Stuttgart
36. Kara F, Karabatak M, Ayyıldız M, Nas E (2020) Effect of machinability, microstructure and hardness of deep cryogenic treatment in hard turning of AISI D2 steel with ceramic cutting. J Mater Res Technol 9(1):969–983. https://doi.org/10.1016/j.jmrt.2019.11.037
37. Eser A, Aşkar Ayyıldız E, Ayyıldız M, Kara F (2021) Artificial intelligence-based surface roughness estimation modelling for milling of AA6061 alloy. Adv Mater Sci Eng. https://doi.org/10.1155/2021/5576600
38. Aydın S, Güdücü Ç, Kutluk F, Öniz A, Özgören M (2019) The impact of musical experience on neural sound encoding performance. Neurosci Lett 694:124–128. https://doi.org/10.1016/j.neulet.2018.11.034
39. Erkan Ö, Işık B, Çiçek A, Kara F (2013) Prediction of damage factor in end milling of glass fibre reinforced plastic composites using artificial neural network. Appl Compos Mater 20(4):517–536. https://doi.org/10.1007/s10443-012-9286-3
40. Li H (1999) An inverse reliability method and its applications in engineering design. Ph.D. thesis, University of British Columbia
41. Červenka V, Jendele L, Červenka J (2012) ATENA program documentation – part 1: theory. Cervenka Consulting, Prague
42. ČSN 73 6222. (2013) Load bearing capacity of road bridges. Prague: Czech Office for Standards, Metrology and Testing. (in Czech)
43. Vořechovský M, Novák D (2009) Correlation control in small-sample Monte Carlo type simulations I: a simulated annealing approach. Probab Eng Mech 24(3):452–462
44. Zimmermann T, Lehký D, Strauss A (2016) Correlation among selected fracture-mechanical parameters of concrete obtained from experiments and inverse analyses. Struct Concrete 17(6):1094–1103